



## The Green's function for the two-dimensional Helmholtz equation in periodic domains

C. M. LINTON

*Department of Mathematical Sciences, Loughborough University, Leicestershire LE11 3TU, U.K.*

Received 7 October 1997; accepted in revised form: 9 March 1998

**Abstract.** Analytical techniques are described for transforming the Green's function for the two-dimensional Helmholtz equation in periodic domains from the slowly convergent representation as a series of images into forms more suitable for computation. In particular methods derived from Kummer's transformation are described, and integral representations, lattice sums and the use of Ewald's method are discussed. Green's functions suitable for problems in parallel-plate acoustic waveguides are also considered and numerical results comparing the accuracy of the various methods are presented.

**Keywords:** Green's functions, periodic domains, waveguides, Helmholtz equation.

### 1. Introduction

A very useful technique for solving scattering problems in which the scatterer is periodic involves the formulation of an integral equation in which the kernel is a periodic Green's function. The numerical solution of this integral equation requires numerous evaluations of the Green's function and so the feasibility of the method is strongly influenced by how efficiently this function can be computed. Unfortunately, standard representations in terms of sums of images usually contain series which converge very slowly and so are unsuitable for numerical work.

Of interest in many branches of physics and engineering is the case of gratings, structures which are periodic in one dimension only, and for such scatterers many problems concerning time-harmonic waves involve the solution of the two-dimensional Helmholtz equation. The literature concerning such problems is vast, see for example [1, 2], and a great deal has been written about the appropriate fundamental solution for such problems.

Information on periodic Green's functions is scattered far and wide, in articles on such diverse topics as electrostatic potentials in crystal lattices and trapped modes in the theory of water waves. Moreover, mathematical conventions used by researchers in different areas often differ widely, making comparison difficult.

This paper attempts to remedy the situation by bringing together, in a consistent notation, the many different analytical techniques that can be used to represent the Green's function in a form suitable for computation. All of the key results in Section 2 have appeared previously, in one guise or another, though the direct application of Ewald's method appears to be new. Also, the formulas for the lattice sums (Equations (2.50) and (2.51) below), although derived nearly 40 years ago, seem to have been overlooked by researchers in this area. Whilst results of numerical computations for each of the methods considered here can also be found in the

literature, the comparison of the accuracy and speed of all the various alternatives, which is given in this paper, is new.

Numerous techniques exist for accelerating slowly-convergent series. Examples include Euler's transformation for alternating series [3, Equation 3.6.27], Shanks transformation [4] and Wynn's algorithm [5]. These methods are general in the sense that they do not take into account the actual form of the terms in the series. Such methods are not discussed in this paper; a survey of them and their use in evaluating periodic sums of three-dimensional point sources is given in [6].

After deriving various alternative expressions for the Green's function in Section 2 we discuss simplifications for the special case of normal incidence in Section 3 and applications to waveguide problems in Section 4. Results of numerical computations comparing the different methods are presented in Section 5.

## 2. Alternative forms for the periodic Green's function

Denote the source point by  $P \equiv (\xi, \eta)$  and the field point by  $Q \equiv (x, y)$ . For convenience we will write  $X = x - \xi$ ,  $Y = y - \eta$  and  $r = (X^2 + Y^2)^{\frac{1}{2}}$ . The Green's function for the Helmholtz equation in an unbounded region satisfies

$$(\nabla^2 + k^2)G = 0, \quad P \neq Q, \quad (2.1)$$

$$G \sim \frac{1}{2\pi} \log r \quad \text{as } kr \rightarrow 0 \quad (2.2)$$

or equivalently, see [7],

$$(\nabla^2 + k^2)G = \delta(X)\delta(Y), \quad (2.3)$$

where  $\delta$  is the Dirac delta function. We also require that as  $kr \rightarrow \infty$ ,  $G \exp(-i\omega t)$  behaves like outgoing circular waves or, in other words, that  $G$  satisfies a Sommerfeld radiation condition. The solution is

$$G = -\frac{i}{4}H_0(kr), \quad (2.4)$$

where, for convenience, we have written  $H_0$  for the Hankel function  $H_0^{(1)}$ .

For an important class of problems involving periodic structures we are led to seek solutions of the form  $\exp(-i\beta y)\psi(x, y)$  where  $\psi$  is periodic in  $y$  with period  $d$ . In a wave diffraction problem  $\exp(-i\beta y)$  then represents the dependence of the incident wave in the direction along the grating and we have  $\beta = k \sin \theta_I$ , where  $\theta_I$  is the angle the incident wave direction makes with the normal to the grating. For such problems the appropriate Green's function, which we label  $G_\beta^d$ , is the solution of (2.3) in a strip of width  $d$  containing the point  $P$  together with the condition that  $\exp(-i\beta y)G_\beta^d$  is periodic in  $y$  with period  $d$ . Equivalently we can define  $G_\beta^d$  to be the solution of

$$(\nabla^2 + k^2)G_\beta^d = \delta(X) \sum_{m=-\infty}^{\infty} \delta(Y - md) e^{im\beta d}. \quad (2.5)$$

For future convenience we define

$$p = \frac{2\pi}{d} \tag{2.6}$$

and, since the sum is over all integers  $m$ , we need only consider  $\beta$  in an interval of length  $p$ . In the case of oblique scattering by a diffraction grating we have  $-k < \beta < k$  with  $\beta = 0$  corresponding to normal incidence, whereas if  $kd < \pi$  then  $k < \beta < p - k$  corresponds to the problem of determining the frequencies of pure Rayleigh–Bloch surface waves along a periodic structure (see [8]). The appropriate condition as  $|X| \rightarrow \infty$  is that  $G_\beta^d \exp(-i\omega t)$  consists of waves travelling away from the line  $X = 0$  if  $-k < \beta < k$ , or is exponentially small if  $k < \beta < p - k$ .

Perhaps the simplest form for  $G_\beta^d$  is a representation as a sum of images, see *e.g.* [9]

$$G_\beta^d(X, Y) = -\frac{i}{4} \sum_{m=-\infty}^{\infty} H_0(kr_m) e^{im\beta d}, \tag{2.7}$$

where

$$r_m = [X^2 + (Y - md)^2]^{\frac{1}{2}}. \tag{2.8}$$

The periodicity requirement is satisfied since

$$\begin{aligned} e^{-i\beta d} G_\beta^d(X, Y + d) &= -\frac{i}{4} \sum_{m=-\infty}^{\infty} H_0(kr_{m-1}) e^{i(m-1)\beta d} \\ &= -\frac{i}{4} \sum_{m=-\infty}^{\infty} H_0(kr_m) e^{im\beta d} = G_\beta^d(X, Y). \end{aligned} \tag{2.9}$$

One problem with (2.7) is that the series converges very slowly (like  $\sum m^{-\frac{1}{2}} \exp(im\theta)$ ) and another is that the asymptotic form as  $|X| \rightarrow \infty$  is not immediately apparent. Some numerical results concerning the application of a standard acceleration procedure to the series in (2.7) are given in [10].

An alternative representation as an eigenfunction expansion can be obtained from (2.7) if we use the Poisson summation formula, which we can formally write as

$$\sum_{m=-\infty}^{\infty} e^{imu} = 2\pi \sum_{m=-\infty}^{\infty} \delta(u + 2m\pi), \tag{2.10}$$

and the integral representation ([11, Equation 2.26]),

$$\begin{aligned} H_0(k(a^2 + b^2)^{\frac{1}{2}}) &= -\frac{2i}{\pi} \int_0^\infty \gamma^{-1} e^{-k\gamma|b|} \cos kat \, dt \\ &= -\frac{i}{\pi} \int_{-\infty}^\infty \gamma^{-1} e^{-k\gamma|b|} e^{-ikat} \, dt. \end{aligned} \tag{2.11}$$

Here

$$\gamma = (t^2 - 1)^{\frac{1}{2}} = -i(1 - t^2)^{\frac{1}{2}}. \tag{2.12}$$

If we substitute (2.11) in (2.7) and then use (2.10), we obtain

$$G_{\beta}^d(X, Y) = -\frac{1}{2d} \sum_{m=-\infty}^{\infty} \frac{e^{-\gamma_m |X|} e^{i\beta_m Y}}{\gamma_m}, \quad (2.13)$$

where we have written

$$\beta_m = \beta + mp, \quad \gamma_m = (\beta_m^2 - k^2)^{\frac{1}{2}} = -i(k^2 - \beta_m^2)^{\frac{1}{2}}. \quad (2.14)$$

In the case  $k < \beta < p - k$  it is clear that  $G_{\beta}^d$  decays exponentially as  $|X| \rightarrow \infty$ , since  $|\beta_m| > k \forall m \in \mathbb{Z}$ , whilst if  $-k < \beta < k$  the form of the Green's function as  $|X| \rightarrow \infty$  is given by

$$G_{\beta}^d(X, Y) \sim -\frac{i}{2kd} \sum_{m=-M}^N \frac{e^{ikt_m |X|} e^{i\beta_m Y}}{t_m}, \quad (2.15)$$

where  $M$  and  $N$  are nonnegative integers such that

$$\beta_{-M-1} < -k < \beta_{-M}, \quad \beta_N < k < \beta_{N+1}, \quad (2.16)$$

and

$$t_m = \left[ 1 - \left( \frac{\beta_m}{k} \right)^2 \right]^{\frac{1}{2}}. \quad (2.17)$$

The derivation of (2.13), often referred to as the spectral representation of the Green's function, from (2.7), the spatial representation, is described variously in, amongst others, [12], [13] and [14]. The form (2.13) can of course be obtained directly rather than from (2.7) and this is done for example, in [15] and [16]. A rigorous derivation of (2.13), using the theory of distributions, can be found in [1]. A disadvantage of (2.13) is that the singularity as  $kr \rightarrow 0$  is not explicit.

#### KUMMER'S TRANSFORMATION

The convergence of the series (2.7) and (2.13) can be improved if we use Kummer's transformation, namely if we convert the slowly convergent series into two series which converge faster by subtracting and adding back a series which has the same asymptotic behaviour as the troublesome series and which can be summed analytically, see [3, Equation 3.6.26].

For  $X = 0$  (2.13) converges very slowly, like (2.7), but we can accelerate the convergence of the series as described in [17]:

$$\begin{aligned} G_{\beta}^d(0, Y) &= -\frac{1}{2d} \sum_{m=-\infty}^{\infty} \frac{e^{i\beta_m Y}}{\gamma_m} \\ &= -\frac{1}{2d} \sum_{m=-\infty}^{\infty} e^{i\beta_m Y} \left( \frac{1}{\gamma_m} - \frac{1}{(\beta_m^2 + k^2)^{\frac{1}{2}}} \right) - \frac{1}{2d} \sum_{m=-\infty}^{\infty} \frac{e^{i\beta_m Y}}{(\beta_m^2 + k^2)^{\frac{1}{2}}}. \end{aligned} \quad (2.18)$$

The terms in the first summation are  $O(|\beta_m|^{-3})$  as  $|m| \rightarrow \infty$  and

$$\begin{aligned} & \frac{1}{2d} \sum_{m=-\infty}^{\infty} \frac{e^{i\beta_m Y}}{(\beta_m^2 + k^2)^{\frac{1}{2}}} \\ &= \frac{e^{i\beta Y}}{4\pi} \sum_{m=-\infty}^{\infty} \int_{-\infty}^{\infty} \frac{e^{-iuY/d} e^{imu}}{[(\beta d - u)^2 + (kd)^2]^{\frac{1}{2}}} du \\ &= \frac{1}{4\pi} \sum_{m=-\infty}^{\infty} e^{im\beta d} \int_{-\infty}^{\infty} \frac{e^{it(Y-md)}}{(t^2 + k^2)^{\frac{1}{2}}} dt = \frac{1}{2\pi} \sum_{m=-\infty}^{\infty} K_0(k|Y - md|) e^{im\beta d}, \end{aligned} \quad (2.19)$$

where we have used (2.10) and an integral representation for the modified Bessel function  $K_0$  given in [18, Equation 8.432(5)]. This final series is exponentially convergent.

For  $|X| > 0$  the terms in the series (2.13) decay like  $|m|^{-1} \exp\{-p|mX|\}$ . Using a different application of Kummer's transformation, described in [19], we can accelerate the convergence of this series. Thus we write

$$G_{\beta}^d(X, Y) = -\frac{e^{i\beta Y}}{2d} \left( \frac{e^{-\gamma_0|X|}}{\gamma_0} + \sum_{m \in \mathbb{Z} \setminus \{0\}} \frac{e^{-\gamma_m|X|} e^{impY}}{\gamma_m} \right). \quad (2.20)$$

Now as  $|m| \rightarrow \infty$ ,

$$\gamma_m = |m|p \left( 1 + \frac{\beta}{mp} - \frac{k^2}{2m^2 p^2} \right) + O(|m|^{-2}), \quad (2.21)$$

$$\gamma_m^{-1} = \frac{1}{|m|p} \left( 1 - \frac{\beta}{mp} + \frac{k^2 + 2\beta^2}{2m^2 p^2} \right) + O(|m|^{-4}), \quad (2.22)$$

from which

$$\gamma_m^{-1} e^{-\gamma_m|X|} = u_m(X) + O(|m|^{-3} e^{-p|mX|}) \quad (2.23)$$

where

$$u_m(X) = \frac{e^{-(|m|p + \text{sgn}(m)\beta)|X|}}{|m|p} \left( 1 - \frac{\beta}{mp} + \frac{k^2|X|}{2|m|p} \right). \quad (2.24)$$

We can then write

$$G_{\beta}^d(X, Y) = -\frac{e^{i\beta Y}}{2d} \left( \frac{e^{-\gamma_0|X|}}{\gamma_0} + S + \sum_{m \in \mathbb{Z} \setminus \{0\}} \left[ \frac{e^{-\gamma_m|X|}}{\gamma_m} - u_m(X) \right] e^{impY} \right) \quad (2.25)$$

where, writing  $Z = |X| + iY$ ,

$$\begin{aligned} S &= \sum_{m \in \mathbb{Z} \setminus \{0\}} u_m(X) e^{impY} \\ &= e^{-\beta|X|} \sum_{m=1}^{\infty} \frac{e^{-mp\bar{Z}}}{mp} \left( 1 - \frac{2\beta - k^2|X|}{2mp} \right) + e^{\beta|X|} \sum_{m=1}^{\infty} \frac{e^{-mpZ}}{mp} \left( 1 + \frac{2\beta + k^2|X|}{2mp} \right). \end{aligned} \quad (2.26)$$

These series can be expressed in closed form in terms of polylogarithms [20]. The polylogarithm function  $\text{Li}_s(z)$ ,  $s \geq 1$ , can be defined by the sum

$$\text{Li}_s(z) = \sum_{m=1}^{\infty} \frac{z^m}{m^s} \quad (2.27)$$

which is valid for  $|z| \leq 1$  except at  $z = 1$  when  $s = 1$ . Clearly  $\text{Li}_1(z) = -\log(1 - z)$ . Thus we have

$$\begin{aligned} S = e^{-\beta|X|} & \left[ \frac{1}{p} \text{Li}_1(e^{-p\bar{Z}}) - \frac{2\beta - k^2|X|}{2p^2} \text{Li}_2(e^{-p\bar{Z}}) \right] \\ & + e^{\beta|X|} \left[ \frac{1}{p} \text{Li}_1(e^{-pZ}) + \frac{2\beta + k^2|X|}{2p^2} \text{Li}_2(e^{-pZ}) \right]. \end{aligned} \quad (2.28)$$

The polylogarithms that appear in this expression can be evaluated quickly and with high accuracy provided  $|Z| < d$  (see [19]). The representation (2.25) includes a sum containing terms which decay like  $|m|^{-3} \exp\{-p|mX|\}$ . This acceleration process can be continued further if we retain more terms in the expansion (2.24). The resulting analysis is straightforward (and, as was pointed out in [21], can be greatly facilitated by the use of a computer algebra package such as MATHEMATICA), and expressions for  $G_\beta^d$  can be obtained containing higher order polylogarithms.

The same idea of adding and subtracting an asymptotically equivalent series can be used to speed up the convergence of (2.7). One method is to introduce a free parameter  $\mu$  and write

$$G_\beta^d(X, Y) = -\frac{i}{4} \sum_{m=-\infty}^{\infty} [H_0(kr_m) - H_0(k\tilde{r}_m)] e^{im\beta d} - \frac{i}{4} \sum_{m=-\infty}^{\infty} H_0(k\tilde{r}_m) e^{im\beta d}, \quad (2.29)$$

where  $\tilde{r}_m = [(X + \mu d)^2 + (Y - md)^2]^{\frac{1}{2}}$ . Since  $H_0(kr_m) \sim H_0(k\tilde{r}_m)$  as  $|m| \rightarrow \infty$ , the first sum converges more rapidly than before (like  $\sum m^{-3/2} \exp(im\theta)$ ) and we can accelerate the second sum by using exactly the same method as was described above to convert (2.7) into (2.13). Thus,

$$G_\beta^d(X, Y) = -\frac{i}{4} \sum_{m=-\infty}^{\infty} [H_0(kr_m) - H_0(k\tilde{r}_m)] e^{im\beta d} - \frac{1}{2d} \sum_{m=-\infty}^{\infty} \frac{e^{-\gamma_m|X+\mu d|} e^{i\beta_m Y}}{\gamma_m}. \quad (2.30)$$

Note that, when  $\mu = 0$ , we recover the eigenfunction expansion (2.13). The parameter  $\mu$  is called a smoothing parameter in [22] and an attenuation constant in a study of related problems involving periodic arrays of three-dimensional point sources [23]. Numerical results are given in [17] which show how the computation of  $G_\beta^d$ , using (2.30), is affected by varying  $\mu$ .

Another way of applying Kummer's transformation to (2.7) is to use the method given in [24]. From [18, Equation 3.411(22)] we have

$$\sum_{m=1}^{\infty} \frac{e^{imu}}{m^{\frac{1}{2}}} = \pi^{-\frac{1}{2}} \int_0^{\infty} \frac{s^{-\frac{1}{2}}}{e^s e^{-iu} - 1} ds \quad (2.31)$$

and hence

$$\begin{aligned} \sum_{m=1}^{\infty} H_0(kr_m) e^{im\beta d} &= \sum_{m=1}^{\infty} \left[ H_0(kr_m) - \left( \frac{2}{\pi m k d} \right)^{\frac{1}{2}} e^{i(mkd - \frac{\pi}{4})} \right] e^{im\beta d} \\ &+ \left( \frac{2}{k d} \right)^{\frac{1}{2}} \frac{e^{-\frac{i\pi}{4}}}{\pi} \int_0^{\infty} \frac{s^{-\frac{1}{2}}}{e^s e^{-i(k+\beta)d} - 1} ds. \end{aligned} \quad (2.32)$$

The terms in the first sum again decay like  $m^{-3/2} \exp(im\theta)$  and the integral is easily evaluated numerically due to the exponential decay of the integrand. If we perform the same analysis on the sum from  $-1$  to  $-\infty$  we are led to the result

$$\begin{aligned} G_{\beta}^d(X, Y) &= -\frac{i}{4} H_0(kr) - \frac{i}{4} \sum_{m \in \mathbb{Z} \setminus \{0\}} \left[ H_0(kr_m) - \left( \frac{2}{\pi |m| k d} \right)^{\frac{1}{2}} e^{i(|m|kd - \frac{\pi}{4})} \right] e^{im\beta d} \\ &- \frac{1+i}{4\pi} \int_0^{\infty} \left[ \frac{1}{e^{-i(k+\beta)d} - e^{-kdu}} + \frac{1}{e^{-i(k-\beta)d} - e^{-kdu}} \right] \frac{e^{-kdu}}{u^{\frac{1}{2}}} du. \end{aligned} \quad (2.33)$$

#### INTEGRAL REPRESENTATIONS

Another method for transforming  $G_{\beta}^d$  into a form more suitable for computation is given in [25]. We begin with the summed geometric progression

$$\sum_{m=1}^{\infty} e^{im(\beta+k)d} e^{-mkdu} = \frac{e^{i(\beta+k)d}}{e^{kdu} - e^{i(\beta+k)d}}, \quad (2.34)$$

multiply by

$$-\frac{2i}{\pi} e^{-ikY} e^{kYu} \frac{\cos[kX(u^2 - 2iu)^{\frac{1}{2}}]}{(u^2 - 2iu)^{\frac{1}{2}}}$$

and integrate with respect to  $u$  from 0 to  $\infty$ . If we then use the result [26, Equation 5.14(16)]

$$e^{-ib} H_0((a^2 + b^2)^{\frac{1}{2}}) = -\frac{2i}{\pi} \int_0^{\infty} \frac{e^{-bu} \cos[a(u^2 - 2iu)^{\frac{1}{2}}]}{(u^2 - 2iu)^{\frac{1}{2}}} du, \quad b \geq 0, \quad (2.35)$$

with  $a = kX$  and  $b = k(md - Y)$ , we obtain

$$\sum_{m=1}^{\infty} H_0(kr_m) e^{im\beta d} = -\frac{2i}{\pi} e^{-ikY} \int_0^{\infty} \frac{e^{k(Y-d)u} \cos[kX(u^2 - 2iu)^{\frac{1}{2}}]}{(e^{-i(\beta+k)d} - e^{-kdu})(u^2 - 2iu)^{\frac{1}{2}}} du \quad (2.36)$$

valid for  $Y \leq d$ . If we replace  $\beta$  by  $-\beta$  and  $Y$  by  $-Y$ , we obtain a similar formula valid for  $Y \geq -d$ . Hence for  $-d \leq Y \leq d$ , from (2.7),

$$\begin{aligned} G_{\beta}^d(X, Y) &= -\frac{i}{4} H_0(kr) - \frac{e^{-ikY}}{2\pi} \int_0^{\infty} \frac{e^{k(Y-d)u} \cos[kX(u^2 - 2iu)^{\frac{1}{2}}]}{(e^{-i(\beta+k)d} - e^{-kdu})(u^2 - 2iu)^{\frac{1}{2}}} du \\ &- \frac{e^{ikY}}{2\pi} \int_0^{\infty} \frac{e^{-k(Y+d)u} \cos[kX(u^2 - 2iu)^{\frac{1}{2}}]}{(e^{i(\beta-k)d} - e^{-kdu})(u^2 - 2iu)^{\frac{1}{2}}} du. \end{aligned} \quad (2.37)$$

The integrals have an integrable singularity at the origin and provided  $|Y| < d$  the integrands decay exponentially as  $u \rightarrow \infty$ .

We can generate an alternative form by making the substitution  $t = (u^2 - 2iu)^{1/2}$ , from which  $u = i + \gamma$  where  $\gamma$  is defined in (2.12). This results in

$$\begin{aligned} G_{\beta}^d(X, Y) &= -\frac{i}{4}H_0(kr) - \frac{1}{2\pi} \int_0^{\infty-i} \frac{e^{k\gamma(Y-d)} \cos kXt}{(e^{-i\beta d} - e^{-k\gamma d})\gamma} dt \\ &\quad - \frac{1}{2\pi} \int_0^{\infty-i} \frac{e^{-k\gamma(Y+d)} \cos kXt}{(e^{i\beta d} - e^{-k\gamma d})\gamma} dt. \end{aligned} \quad (2.38)$$

The integrands have poles on the real  $t$ -axis, but the path of integration can be still be deformed back onto the real axis, provided we indent the contour to pass beneath the poles. Thus, we can write

$$\begin{aligned} G_{\beta}^d(X, Y) &= -\frac{i}{4}H_0(kr) - \frac{1}{2\pi} \\ &\quad \times \int_0^{\infty} \left[ \frac{e^{k\gamma Y}}{(e^{-i\beta d} - e^{-k\gamma d})} + \frac{e^{-k\gamma Y}}{(e^{i\beta d} - e^{-k\gamma d})} \right] \frac{e^{-k\gamma d}}{\gamma} \cos kXt dt \\ &= -\frac{i}{4}H_0(kr) - \frac{1}{2\pi} \\ &\quad \times \int_0^{\infty} \frac{(\cos \beta d - e^{-k\gamma d}) \cosh k\gamma Y + i \sin \beta d \sinh k\gamma Y}{\gamma (\cosh k\gamma d - \cos \beta d)} \cos kXt dt \end{aligned} \quad (2.39)$$

$$= -\frac{1}{2\pi} \int_0^{\infty} \frac{e^{i\beta d \operatorname{sgn}(Y)} \sinh k\gamma |Y| + \sinh k\gamma (d - |Y|)}{\gamma (\cosh k\gamma d - \cos \beta d)} \cos kXt dt \quad (2.40)$$

using (2.11). This is precisely the same form as that derived directly from the governing equations in [27] and the transformation used to take (2.37) into (2.39) is just the reverse of that used in [28]. It is straightforward to recover the far-field form (2.15) from the representation (2.39), since, when  $|\beta| < k$ , the integrand has poles on the real axis at  $t = t_m$ ,  $m = -M, \dots, N$  where  $M, N$  and  $t_m$  are given by (2.16) and (2.17).

If  $k < \beta < p - k$ , there is no difficulty in evaluating the integrals in (2.39) and (2.40), whilst if  $|\beta| < k$ , they can be evaluated efficiently if we use the method described in [11]. We begin by writing the contour integral as the sum of a Cauchy principal-value integral and the contributions from the poles on the real axis (which can be evaluated explicitly). The integral is then of the form

$$\int_0^{\infty} \frac{f(t)}{g(t)} dt,$$

where  $g(t)$  has simple zeros at  $t = t_m$ ,  $m = -M, \dots, N$ , and for which  $f(t_m) \neq 0$ . If we write  $\tau = \max t_m$ , then

$$\begin{aligned} \int_0^{\infty} \frac{f(t)}{g(t)} dt &= \int_{2\tau}^{\infty} \frac{f(t)}{g(t)} dt + \int_0^{2\tau} \left[ \frac{f(t)}{g(t)} - \sum_{m=-M}^N \frac{f(t_m)}{g'(t_m)(t - t_m)} \right] dt \\ &\quad + \sum_{m=-M}^N \frac{f(t_m)}{g'(t_m)} \log \left( \frac{2\tau}{t_m} - 1 \right). \end{aligned} \quad (2.41)$$



The integrand in the second integral is integrable throughout the range of integration, though care must be taken near to the points  $t = t_m$ , since at these points the integrand is the difference between two large numbers.

We can demonstrate the equivalence of (2.7) and (2.40) directly, if we make use of the geometrical series identity

$$\sum_{m=-\infty}^{\infty} e^{im\beta d} e^{-k\gamma|Y-md|} = \frac{e^{i\beta d \operatorname{sgn}(Y)} \sinh k\gamma|Y| + \sinh k\gamma(d - |Y|)}{\cosh k\gamma d - \cos \beta d}, \quad (2.42)$$

valid for  $|Y| < d$ , which was used in [29] to derive rapidly convergent series for the electric potential within a general crystal lattice. If we substitute this in (2.40) and use (2.11) we immediately obtain (2.7).

An integral representation equivalent to (2.38) has been obtained by Cadilhac and is quoted in [21], though the derivation remains unpublished. This representation was used in [30] and significant computational savings were reported over methods derived from Kummer's transformation.

#### LATTICE SUMS

Another representation for  $G_\beta^d$  can be derived in terms of so-called lattice sums (which for our problem are Schlömilch series) as described in [19] for  $\beta = 0$  and in [31] for general  $\beta$ . Graf's addition theorem for Bessel functions [18, Equation 8.530(2)] can be used to express (2.7) solely in terms of the polar coordinates  $(r, \theta)$  where  $X = r \cos \theta$ ,  $Y = r \sin \theta$ . Thus, provided  $r < d$ , we can write

$$G_\beta^d(X, Y) = -\frac{i}{4} \left[ H_0(kr) + \sum_{m \in \mathbb{Z} \setminus \{0\}} e^{im\beta d} \sum_{\ell=-\infty}^{\infty} J_\ell(kr) H_\ell(|m|kd) e^{i\ell\phi_m} e^{i\ell(\frac{\pi}{2}-\theta)} \right], \quad (2.43)$$

where

$$\phi_m = \begin{cases} \pi & \text{if } m < 0 \\ 0 & \text{if } m > 0. \end{cases} \quad (2.44)$$

The lattice sums  $S_\ell(\beta d, kd)$  are defined by

$$S_\ell(\beta d, kd) = \sum_{m \in \mathbb{Z} \setminus \{0\}} e^{im\beta d} H_\ell(|m|kd) e^{i\ell\phi_m} = \sum_{m=1}^{\infty} H_\ell(mkd) (e^{im\beta d} + (-1)^\ell e^{-im\beta d}) \quad (2.45)$$

and the Green's function can then be expressed as

$$G_\beta^d(X, Y) = -\frac{i}{4} \left[ H_0(kr) + \sum_{\ell=0}^{\infty} \epsilon_\ell S_\ell J_\ell(kr) \cos \ell \left( \frac{\pi}{2} - \theta \right) \right], \quad (2.46)$$

where  $\epsilon_0 = 1$ ,  $\epsilon_\ell = 2$  for  $\ell > 0$ . We have  $H_\ell(mkd) J_\ell(kr) \sim -i(\pi\ell)^{-1}(r/md)^\ell$  as  $\ell \rightarrow \infty$  [3, Equation 9.3.1] and so the summation converges exponentially. Also the lattice sums themselves only have to be evaluated once as they do not depend on the position at which  $G_\beta^d$

is computed. However, the computation of  $S_\ell$  must be performed with care since  $S_\ell$  becomes very large and  $J_\ell$  very small as  $\ell$  increases.

Algorithms for the computation of the lattice sums  $S_\ell$ , the real and imaginary parts of which are evaluated separately, are given in [31]. In that paper numerical results are presented for the calculation of the Green's function which suggest that (2.46) can be computationally competitive in situations where the value of  $G_\beta^d$  is required at a large number of points. The formulas given for the real parts are in terms of finite sums and correspond to those given in [32] (see below), but those for the imaginary parts seem unnecessarily complex in view of Twersky's results. For  $\ell = 0$  we have (see [31])

$$S_0 = -1 - \frac{2i}{\pi} \left[ C + \log \frac{k}{2p} \right] - \frac{2i}{\gamma_0 d} - \frac{2i}{d} \sum_{m \in \mathbb{Z} \setminus \{0\}} \left( \frac{1}{\gamma_m} - \frac{1}{p|m|} \right), \tag{2.47}$$

where  $C \approx 0.5772157$  is Euler's constant. The convergence of the sum can be improved if we use Kummer's transformation. Thus from (2.22), noting that

$$\sum_{m \in \mathbb{Z} \setminus \{0\}} \frac{1}{m|m|} = 0, \tag{2.48}$$

we obtain

$$S_0 = -1 - \frac{2i}{\pi} \left[ C + \log \frac{k}{2p} \right] - \frac{2i}{\gamma_0 d} - \frac{2i(k^2 + 2\beta^2)}{p^3 d} \zeta(3) - \frac{2i}{d} \sum_{m \in \mathbb{Z} \setminus \{0\}} \left( \frac{1}{\gamma_m} - \frac{1}{p|m|} - \frac{k^2 + 2\beta^2}{2p^3|m|^3} \right), \tag{2.49}$$

where  $\zeta(s)$  is the Riemann zeta function and  $\zeta(3) \approx 1.2020569$  [3, Section 23.2]. The terms in the sum are  $O(|m|^{-4})$  as  $|m| \rightarrow \infty$ .

For  $\ell > 0$  Twersky gives

$$S_{2\ell} = -\frac{2i}{d} \sum_{m=0}^{\infty} \frac{e^{-2i\ell\theta_m}}{\gamma_m} - \frac{2i}{d} \sum_{m=-1}^{-\infty} \frac{e^{2i\ell\theta_m}}{\gamma_m} + \frac{i}{\ell\pi} + \frac{i}{\pi} \sum_{m=1}^{\ell} \frac{(-1)^m 2^{2m} (\ell + m - 1)!}{(2m)! (\ell - m)!} \left( \frac{p}{k} \right)^{2m} B_{2m}(\beta/p), \tag{2.50}$$

$$S_{2\ell-1} = \frac{2i}{d} \sum_{m=0}^{\infty} \frac{e^{-i(2\ell-1)\theta_m}}{\gamma_m} - \frac{2i}{d} \sum_{m=-1}^{-\infty} \frac{e^{i(2\ell-1)\theta_m}}{\gamma_m} - \frac{2}{\pi} \sum_{m=0}^{\ell-1} \frac{(-1)^m 2^{2m} (\ell + m - 1)!}{(2m + 1)! (\ell - m - 1)!} \left( \frac{p}{k} \right)^{2m+1} B_{2m+1}(\beta/p), \tag{2.51}$$

where

$$\theta_m = \sin^{-1}(\beta_m/k) \tag{2.52}$$

and  $B_m(x)$  is the Bernoulli polynomial, which can be written as a finite sum [3, Equation 23.1.7]. The value of  $\theta_m$  is taken so that if  $|\beta_m| < k$ ,  $|\theta_m| \leq \pi/2$ , whereas if  $m > N$  (see (2.16))  $\text{Re}(\theta_m) = \pi/2$ ,  $\text{Im}(\theta_m) < 0$  and if  $m < -M$ ,  $\text{Re}(\theta_m) = -\pi/2$ ,  $\text{Im}(\theta_m) > 0$ .

The infinite sums in (2.50) and (2.51) converge fairly slowly for small  $\ell$ , but can be accelerated if we use Kummer's transformation as was done for  $S_0$ . We obtain

$$\begin{aligned}
 S_{2\ell} = & -\frac{2i e^{-2i\ell\theta_0}}{\gamma_0 d} - 2i \sum_{m=1}^{\infty} \left\{ \frac{e^{-2i\ell\theta_m}}{\gamma_m d} + \frac{e^{2i\ell\theta_{-m}}}{\gamma_{-m} d} - \frac{(-1)^\ell}{m\pi} \left(\frac{k}{2mp}\right)^{2\ell} \right\} \\
 & - \frac{2i(-1)^\ell}{\pi} \left(\frac{k}{2p}\right)^{2\ell} \zeta(2\ell + 1) + \frac{i}{\ell\pi} \\
 & + \frac{i}{\pi} \sum_{m=1}^{\ell} \frac{(-1)^m 2^{2m} (\ell + m - 1)!}{(2m)! (\ell - m)!} \left(\frac{p}{k}\right)^{2m} B_{2m}(\beta/p), \tag{2.53}
 \end{aligned}$$

$$\begin{aligned}
 S_{2\ell-1} = & \frac{2i e^{-i(2\ell-1)\theta_0}}{\gamma_0 d} + 2i \sum_{m=1}^{\infty} \left\{ \frac{e^{-i(2\ell-1)\theta_m}}{\gamma_m d} - \frac{e^{i(2\ell-1)\theta_{-m}}}{\gamma_{-m} d} + \frac{i(-1)^\ell \beta d \ell}{m^2 \pi^2} \left(\frac{k}{2mp}\right)^{2\ell-1} \right\} \\
 & + \frac{2(-1)^\ell \beta d \ell}{\pi^2} \left(\frac{k}{2p}\right)^{2\ell-1} \zeta(2\ell + 1) \\
 & - \frac{2}{\pi} \sum_{m=0}^{\ell-1} \frac{(-1)^m 2^{2m} (\ell + m - 1)!}{(2m + 1)! (\ell - m - 1)!} \left(\frac{p}{k}\right)^{2m+1} B_{2m+1}(\beta/p). \tag{2.54}
 \end{aligned}$$

The slowest convergence occurs in  $S_1$  and  $S_2$  in which the terms are  $O(m^{-5})$  as  $m \rightarrow \infty$ . This acceleration procedure can of course be repeated and the infinite sums in (2.49), (2.53) and (2.54) written as sums of more rapidly convergent series together with more evaluations of the Riemann zeta function with odd integer arguments.

#### EWALD'S METHOD

A very elegant procedure for the evaluation of the Green's function associated with the Helmholtz equation on a periodic structure was devised by Ewald [33] and is used extensively in the analysis of crystal lattices. This procedure is usually described in the literature in the context of three-dimensional lattices, see *e.g.* [34], and occasionally for two-dimensional lattices, as in [35]. Furthermore the procedure is usually applied to the case where three-dimensional point sources are distributed throughout the lattice rather than the situation relevant to the present paper, namely line sources distributed over a one-dimensional lattice. An expression for  $G_\beta^d$  found by integrating the result of [35] is given in [25], but a direct application of Ewald's method to the Green's function  $G_\beta^d$  does not appear to exist in the literature.

The underlying idea behind the method, which is somewhat obscured by the technicalities of its application, is as follows. Consider a function  $f(x)$  which decays slowly as  $|x| \rightarrow \infty$ . Then for any function  $F(x)$  we can write

$$f(x) = f(x)F(x) + \frac{1}{\sqrt{2\pi}} \int_{-\infty}^{\infty} e^{i\omega x} \tilde{G}(\omega) d\omega, \tag{2.55}$$

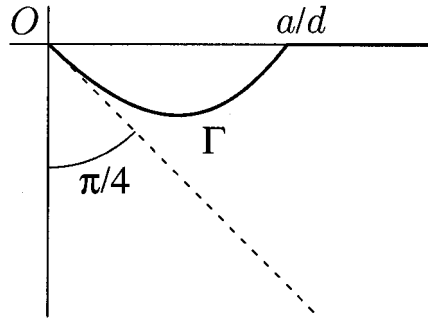


Figure 1. Deformed contour for the integral representation of the Hankel function used in Ewald's method.

where  $\tilde{G}$  is the Fourier transform of  $G(x) = f(x)(1 - F(x))$ . If we chose  $F$  so that  $f(x)F(x)$  tends to zero rapidly as  $|x| \rightarrow \infty$  then  $G(x)$  will tend to zero slowly and hence its Fourier transform  $\tilde{G}(\omega)$  will decay rapidly as  $|\omega| \rightarrow \infty$ . In fact Ewald considered the three-dimensional analogue of (2.55) and for the fundamental electrostatic source potential  $f(r) = 1/r$  took  $F(r) = \operatorname{erfc}(ar)$ , where  $a$  is an arbitrary positive convergence parameter and  $\operatorname{erfc}(z) \sim \pi^{-1/2}z^{-1} \exp[-z^2]$ ,  $|\arg z| < 3\pi/4$ , is the complementary error function. Other forms for  $F$  are possible of course, and a number of variations to the Ewald transform for the potential  $1/r$  are given in [36]. An obvious choice is to take  $F$  to be identically zero and then Ewald's method reduces to taking the Fourier transform, which is equivalent to the process of transforming (2.7) into (2.13).

As was pointed out in [37], Ewald's method applied to three-dimensional point sources derives from an integral representation for the function  $H_{-1/2}(kr) \equiv (2/\pi kr)^{1/2} \exp\{ikr\}$  and so to apply the method in our case we begin with the equivalent representation for  $H_0(kr)$ . Thus after a change of variable [18, Equation 8.421(8)] becomes

$$H_0(kr) = -\frac{2i}{\pi} \int_0^\infty \exp[-i\pi/4] u^{-1} e^{-r^2 u^2} e^{k^2/4u^2} du. \quad (2.56)$$

In the analysis which follows we assume that  $k$  has a small positive imaginary part, but the final result is valid for real  $k$  by analytical continuation. In (2.56) the contour is the line  $\arg u = -\pi/4$  and this can be deformed into two parts,  $\Gamma$  and  $(a/d, \infty)$ , where  $a$  is an arbitrary positive constant, as shown in Figure 1.

This integral representation can be substituted in (2.7) and we obtain  $G_\beta^d = G_1 + G_2$  where

$$G_1 = -\frac{1}{2\pi} \int_\Gamma u^{-1} e^{-X^2 u^2} e^{k^2/4u^2} \sum_{m=-\infty}^{\infty} e^{im\beta d} e^{-(Y-md)^2 u^2} du, \quad (2.57)$$

$$G_2 = -\frac{1}{4\pi} \sum_{m=-\infty}^{\infty} e^{im\beta d} \int_1^\infty u^{-1} e^{-a^2 r_m^2 u/d^2} e^{k^2 d^2/4a^2 u} du. \quad (2.58)$$

In order to write  $G_1$  in a convenient form we consider the function

$$f(Y) = e^{-i\beta Y} \sum_{m=-\infty}^{\infty} e^{im\beta d} e^{-(Y-md)^2 u^2} \quad (2.59)$$

which is periodic with period  $d$  and hence can be expanded as a Fourier series. Thus

$$f(Y) = \sum_{n=-\infty}^{\infty} a_n e^{2\pi i n Y/d}, \quad (2.60)$$

where

$$\begin{aligned} a_n &= \frac{1}{d} \int_0^d f(Y) e^{-2\pi i n Y/d} dY = \frac{1}{d} \sum_{m=-\infty}^{\infty} e^{i m \beta d} \int_0^d e^{-i \beta_n Y} e^{-(Y-md)^2 u^2} dY \\ &= \frac{1}{d} \sum_{m=-\infty}^{\infty} e^{i m d(\beta - \beta_n)} \int_{-md}^{-md+d} e^{-i \beta_n s} e^{-s^2 u^2} ds = \frac{1}{d} \int_{-\infty}^{\infty} e^{-i \beta_n s} e^{-s^2 u^2} ds \\ &= \frac{e^{-\beta_n^2/4u^2}}{d} \int_{-\infty}^{\infty} e^{-u^2(s+i\beta_n/2u^2)^2} ds = \frac{\pi^{\frac{1}{2}}}{ud} e^{-\beta_n^2/4u^2} \end{aligned} \quad (2.61)$$

provided  $|\arg u| < \pi/4$  which is the case for all  $u$  on  $\Gamma$ . Note that  $f(Y)$  is a theta function and the derivation of (2.60), (2.61) corresponds to Jacobi's imaginary transformation, [38, Section 21.51].

The Fourier series for  $f(Y)$ , (2.60), can now be substituted in the expression (2.57) for  $G_1$  resulting in

$$G_1 = -\frac{1}{2\pi^{\frac{1}{2}}d} \sum_{m=-\infty}^{\infty} e^{i\beta_m Y} \int_{\Gamma} u^{-2} e^{-X^2 u^2} e^{-\gamma_m^2/4u^2} du \quad (2.62)$$

where  $\gamma_m$  is defined in (2.14). Now we make the change of variable  $u = 1/s$  so that

$$G_1 = -\frac{1}{2\pi^{\frac{1}{2}}d} \sum_{m=-\infty}^{\infty} e^{i\beta_m Y} \int_{d/a}^{\infty} \exp[i\pi/4] e^{-X^2/s^2} e^{-\gamma_m^2 s^2/4} ds. \quad (2.63)$$

If  $\gamma_m^2 > 0$  the contour of integration can be deformed back to the real axis, whereas if  $\gamma_m^2 < 0$  the change of variable  $s = it$  leads to an integral from  $-id/a$  to  $\infty \exp[-i\pi/4]$  which can be deformed into an integral from  $-id/a$  to  $\infty$ . In either case an application of [3, Equation 7.4.34], shows that

$$G_1 = -\frac{1}{4d} \sum_{m=-\infty}^{\infty} \frac{e^{i\beta_m Y}}{\gamma_m} \left[ e^{\gamma_m X} \operatorname{erfc} \left( \frac{\gamma_m d}{2a} + \frac{aX}{d} \right) + e^{-\gamma_m X} \operatorname{erfc} \left( \frac{\gamma_m d}{2a} - \frac{aX}{d} \right) \right]. \quad (2.64)$$

The final exponential in the expression for  $G_2$  can be expanded as a power series and hence we obtain the following expression for the periodic Green's function:

$$\begin{aligned} G_{\beta}^d(X, Y) &= -\frac{1}{4d} \sum_{m=-\infty}^{\infty} \frac{e^{i\beta_m Y}}{\gamma_m} \left[ e^{\gamma_m X} \operatorname{erfc} \left( \frac{\gamma_m d}{2a} + \frac{aX}{d} \right) + e^{-\gamma_m X} \operatorname{erfc} \left( \frac{\gamma_m d}{2a} - \frac{aX}{d} \right) \right] \\ &\quad - \frac{1}{4\pi} \sum_{m=-\infty}^{\infty} e^{i m \beta d} \sum_{n=0}^{\infty} \frac{1}{n!} \left( \frac{kd}{2a} \right)^{2n} E_{n+1} \left( \frac{a^2 r_m^2}{d^2} \right), \end{aligned} \quad (2.65)$$

where  $E_n(x) = \int_1^\infty u^{-n} e^{-xu} du \sim x^{-1} e^{-x}$  as  $x \rightarrow \infty$  is the exponential integral.

The constant  $a$  in this expression is positive but otherwise arbitrary and by varying  $a$  the convergence of the two series is affected. Increasing  $a$  causes the second summation to converge faster and the first slower. A discussion of the considerations relevant to the choice of  $a$  is given in [25]. The numerical evaluation of the exponential integral presents no problems and the same applies to the complementary error function when the argument is real. An efficient algorithm for computing  $\text{erfc}(z)$  is given in [39].

### 3. Normal incidence

When  $\beta = 0$ , corresponding to normal incidence, some of the preceding expressions for  $G$  simplify considerably. Thus, since from (2.14)  $\gamma_m = \gamma_{-m} = (m^2 p^2 - k^2)^{1/2}$  when  $\beta = 0$ , (2.13) becomes

$$G_0^d(X, Y) = -\frac{1}{2d} \sum_{m=0}^{\infty} \frac{\epsilon_m}{\gamma_m} e^{-\gamma_m |X|} \cos mpY, \quad (3.1)$$

and

$$G_0^d(X, Y) \sim -\frac{i}{2kd} \sum_{m=0}^M \frac{\epsilon_m}{t_m} e^{ikt_m |X|} \cos mpY, \quad (3.2)$$

where  $M$  is a nonnegative integer such that  $Mp < k < (M+1)p$ .

The integral representations (2.37), (2.39) and (2.40) reduce to

$$G_0^d(X, Y) = -\frac{i}{4} H_0(kr) - \frac{1}{\pi} \int_0^\infty \frac{\cosh[kY(u-i)] \cos[kX(u^2 - 2iu)^{1/2}]}{(e^{kd(u-i)} - 1)(u^2 - 2iu)^{1/2}} du \quad (3.3)$$

$$= -\frac{i}{4} H_0(kr) - \frac{1}{\pi} \int_0^\infty \frac{\cosh k\gamma Y \cos kXt}{\gamma(e^{k\gamma d} - 1)} dt \quad (3.4)$$

$$= \frac{1}{2\pi} \int_0^\infty \left( \sinh k\gamma |Y| - \coth \frac{k\gamma d}{2} \cosh k\gamma Y \right) \frac{\cos kXt}{\gamma} dt. \quad (3.5)$$

From (2.45) we see that the lattice sums  $S_\ell(0, kd)$ ,  $\ell \in \mathbb{N} \cup \{0\}$ , satisfy

$$S_{2\ell}(0, kd) = 2 \sum_{m=1}^{\infty} H_{2\ell}(mkd), \quad S_{2\ell+1}(0, kd) = 0, \quad (3.6)$$

and the Green's function can then be expressed as

$$G_0^d(X, Y) = -\frac{i}{4} \left[ H_0(kr) + \sum_{\ell=0}^{\infty} (-1)^\ell \epsilon_\ell S_{2\ell} J_{2\ell}(kr) \cos 2\ell\theta \right]. \quad (3.7)$$

Now  $S_0$  is given by (2.49) with  $\beta = 0$  and from (2.50)

$$S_{2\ell} = -\frac{2i}{d} \sum_{m=0}^{\infty} \epsilon_m \frac{e^{-2i\ell\theta_m}}{\gamma_m} + \frac{i}{\ell\pi} + \frac{i}{\pi} \sum_{m=1}^{\ell} \frac{(-1)^m 2^{2m} (\ell+m-1)!}{(2m)! (\ell-m)!} \left(\frac{p}{k}\right)^{2m} B_{2m}, \quad (3.8)$$

where  $B_{2m} \equiv B_{2m}(0)$  are the Bernoulli numbers.

For  $\beta = 0$ , Ewald's method gives

$$\begin{aligned}
 G_0^d(X, Y) = & -\frac{1}{4d} \sum_{m=0}^{\infty} \epsilon_m \frac{\cos mpY}{\gamma_m} \\
 & \times \left[ e^{\gamma_m X} \operatorname{erfc} \left( \frac{\gamma_m d}{2a} + \frac{aX}{d} \right) + e^{-\gamma_m X} \operatorname{erfc} \left( \frac{\gamma_m d}{2a} - \frac{aX}{d} \right) \right] \\
 & - \frac{1}{4\pi} \sum_{m=0}^{\infty} \epsilon_m \sum_{n=0}^{\infty} \frac{1}{n!} \left( \frac{kd}{2a} \right)^{2n} E_{n+1} \left( \frac{a^2 r_m^2}{d^2} \right). \tag{3.9}
 \end{aligned}$$

It is also worth noting that simplifications also arise when  $\beta = \pi/d$ . Thus for this value of  $\beta$  we have  $\gamma_m = \gamma_{-m-1} = [(m + \frac{1}{2})^2 p^2 - k^2]^{1/2}$  and hence, from (2.13),

$$G_{\pi/d}^d(X, Y) = -\frac{1}{d} \sum_{m=0}^{\infty} \frac{e^{-\gamma_m |X|}}{\gamma_m} \cos(m + \frac{1}{2})pY. \tag{3.10}$$

We also have

$$G_{\pi/d}^d(X, Y) = G_0^{2d}(X, Y) - G_0^{2d}(X, Y - d) \tag{3.11}$$

which can be derived very simply from (2.7). The relationship between problems in which  $\beta = 0$  and  $\beta = \pi/d$  (when  $kd < \pi$ ) has been utilized previously in [8] and [40] to show that as  $\beta \rightarrow \pi/d$  pure Rayleigh–Bloch surface waves along certain periodic gratings go over to channel trapped modes.

#### 4. Waveguide problems

For scattering problems in a parallel-plate waveguide of width  $d$  it is appropriate to consider a Green's function which, rather than being periodic, satisfies given boundary conditions on  $y = 0$  and  $y = d$  and which are singular at  $(\xi, \eta)$  where  $0 < \eta < d$ . Below we will consider the case of Neumann and Dirichlet boundary conditions, corresponding to acoustically hard and soft boundaries, and denote the Green's functions for these problems by  $G_N^d$  and  $G_D^d$  respectively. Thus

$$\frac{\partial G_N^d}{\partial y} = 0 \quad \text{and} \quad G_D^d = 0 \quad \text{on } y = 0, d. \tag{4.1}$$

We will also consider the case of a Green's function which satisfies a Dirichlet condition on  $y = 0$  and a Neumann condition on  $y = d$ . Such a Green's function, which we will denote by  $G_M^d$ , has been used for the determination of trapped mode frequencies in perturbed waveguides, see [41]. Thus

$$G_M^d = 0 \quad \text{on } y = 0, \tag{4.2}$$

$$\frac{\partial G_M^d}{\partial y} = 0 \quad \text{on } y = d. \tag{4.3}$$

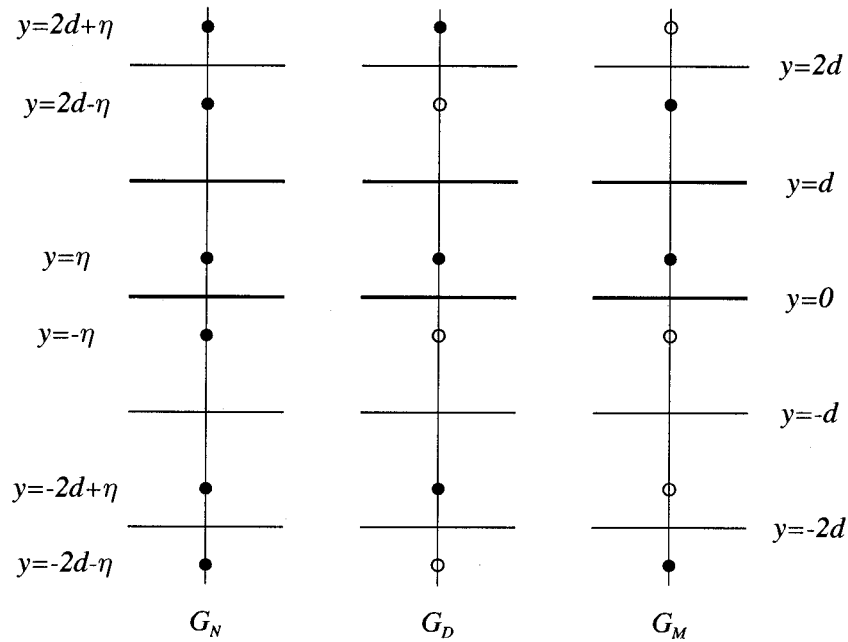


Figure 2. Image distributions for  $G_N$ ,  $G_D$  and  $G_M$ . The solid circles represent sources,  $-\frac{1}{4}H_0(kr)$ , and the open circles represent sinks,  $\frac{1}{4}H_0(kr)$ , where  $r$  is the distance from the singularity.

All these Green's functions can be expressed in terms of the periodic Green's function. We have

$$G_N^d(X, y, \eta) = G_0^{2d}(X, y - \eta) + G_0^{2d}(X, y + \eta), \tag{4.4}$$

$$G_D^d(X, y, \eta) = G_0^{2d}(X, y - \eta) - G_0^{2d}(X, y + \eta), \tag{4.5}$$

$$G_M^d(X, y, \eta) = G_D^{2d}(X, y, \eta) - G_D^{2d}(X, y - 2d, \eta), \tag{4.6}$$

$$= G_{\pi/2d}^{2d}(X, y - \eta) - G_{\pi/2d}^{2d}(X, y + \eta), \tag{4.7}$$

which, since  $G_0^d(X, Y) = G_0^d(X, -Y)$ , can easily be shown to satisfy the appropriate boundary conditions listed above. The distribution of images that these correspond to is shown in Figure 2.

From (2.13) we obtain the eigenfunction expansions

$$G_N^d(X, y, \eta) = -\frac{1}{2} \sum_{m=0}^{\infty} \epsilon_m \frac{e^{-\alpha_{2m}|X|/d}}{\alpha_{2m}} \cos \frac{m\pi y}{d} \cos \frac{m\pi \eta}{d}, \tag{4.8}$$

$$G_D^d(X, y, \eta) = -\sum_{m=1}^{\infty} \frac{e^{-\alpha_{2m}|X|/d}}{\alpha_{2m}} \sin \frac{m\pi y}{d} \sin \frac{m\pi \eta}{d}, \tag{4.9}$$

$$G_M^d(X, y, \eta) = -\sum_{m=1}^{\infty} \frac{e^{-\alpha_{2m-1}|X|/d}}{\alpha_{2m-1}} \sin \frac{(m - \frac{1}{2})\pi y}{d} \sin \frac{(m - \frac{1}{2})\pi \eta}{d}, \tag{4.10}$$



where we have written

$$\alpha_m = \left( \frac{m^2 \pi^2}{4} - k^2 d^2 \right)^{\frac{1}{2}} = -i \left( k^2 d^2 - \frac{m^2 \pi^2}{4} \right)^{\frac{1}{2}}. \quad (4.11)$$

Kummer's transformation can be used to accelerate all these series. For example, in exactly the same way as (2.25) was obtained we can derive the result

$$G_D^d(X, y, \eta) = -S + \sum_{m=1}^{\infty} \left[ \frac{e^{-\alpha_{2m}|X|/d}}{\alpha_{2m}} - v_m(X) \right] \sin \frac{m\pi y}{d} \sin \frac{m\pi \eta}{d}, \quad (4.12)$$

where

$$v_m(X) = \frac{e^{-m\pi|X|/d}}{m\pi} \left( 1 + \frac{k^2|X|d}{2m\pi} \right) \quad (4.13)$$

and

$$S = \frac{1}{4\pi} \left[ \text{Li}_1(e^{-\pi Z_+/d}) + \text{Li}_1(e^{-\pi \bar{Z}_+/d}) - \text{Li}_1(e^{-\pi Z_-/d}) - \text{Li}_1(e^{-\pi \bar{Z}_-/d}) \right. \\ \left. + \frac{k^2|X|d}{2\pi} (\text{Li}_2(e^{-\pi Z_+/d}) + \text{Li}_2(e^{-\pi \bar{Z}_+/d}) - \text{Li}_2(e^{-\pi Z_-/d}) - \text{Li}_2(e^{-\pi \bar{Z}_-/d})) \right], \quad (4.14)$$

where  $Z_{\pm} = |X| + i(y \pm \eta)$ .

The calculation of  $G_N$ ,  $G_D$  and  $G_M$  by the use of lattice sums is straightforward since the lattice sums themselves do not depend on the source or field point. Hence (3.7) can easily be substituted in the right-hand sides of (4.4)–(4.6). For example

$$G_N^d(X, y, \eta) = -\frac{i}{4} \left[ H_0(kr) + H_0(kr') \right. \\ \left. + \sum_{\ell=0}^{\infty} (-1)^{\ell} \epsilon_{\ell} S_{2\ell}(0, 2kd) (J_{2\ell}(kr) \cos 2\ell\theta + J_{2\ell}(kr') \cos 2\ell\theta') \right], \quad (4.15)$$

where  $(r', \theta')$  are polar coordinates centred on the point  $(\xi, -\eta)$ , i.e.  $X = r' \cos \theta'$  and  $y + \eta = r' \sin \theta'$ .

If we substitute the integral representations of the normal incidence Green's function, Equations (3.3)–(3.5), in (4.4) we obtain

$$G_N^d(X, y, \eta) = -\frac{i}{4} [H_0(kr) + H_0(kr')] \\ - \frac{2}{\pi} \int_0^{\infty} \frac{\cosh[ky(u-i)] \cosh[k\eta(u-i)] \cos[kX(u^2 - 2iu)^{\frac{1}{2}}]}{(e^{2kd(u-i)} - 1)(u^2 - 2iu)^{\frac{1}{2}}} du \quad (4.16)$$

$$= -\frac{i}{4} [H_0(kr) + H_0(kr')] - \frac{2}{\pi} \int_0^{\infty} \frac{\cosh k\gamma y \cosh k\gamma \eta}{\gamma (e^{2k\gamma d} - 1)} \cos kXt dt \quad (4.17)$$

$$= \frac{1}{\pi} \int_0^{\infty} (\sinh k\gamma y_{>} - \coth k\gamma d \cosh k\gamma y_{>}) \cosh k\gamma y_{<} \frac{\cos kXt}{\gamma} dt. \quad (4.18)$$

Here  $y_< = \min(y, \eta)$  and  $y_> = \max(y, \eta)$ . The second Hankel function in (4.16) and (4.17) can of course be incorporated into the integral if we use (2.11). Similarly, we can derive

$$G_D^d(X, y, \eta) = -\frac{i}{4}[H_0(kr) - H_0(kr')] + \frac{2}{\pi} \int_0^\infty \frac{\sinh[ky(u-i) \sinh[k\eta(u-i)] \cos[kX(u^2 - 2iu)^{\frac{1}{2}}]}{(e^{2kd(u-i)} - 1)(u^2 - 2iu)^{\frac{1}{2}}} du \quad (4.19)$$

$$= -\frac{i}{4}[H_0(kr) - H_0(kr')] + \frac{2}{\pi} \int_0^\infty \frac{\sinh k\gamma y \sinh k\gamma \eta}{\gamma(e^{2k\gamma d} - 1)} \cos kXt dt \quad (4.20)$$

$$= -\frac{1}{\pi} \int_0^\infty (\cosh k\gamma y_> - \coth k\gamma d \sinh k\gamma y_>) \sinh k\gamma y_< \frac{\cos kXt}{\gamma} dt \quad (4.21)$$

and these formulas can be used to construct corresponding expressions for  $G_M^d$  from (4.6)

## 5. Numerical results

There are many factors which influence the choice of method for the computation of the Green's function in a given situation. Which method is the best will depend on the accuracy required, the number of evaluations to be made, the values of the non-dimensional parameters  $X/d, Y/d, kd$  and  $\beta d$ , the presence or otherwise of programs for computing the necessary special functions, and so on. The numerical results below cannot therefore provide all the information necessary in order to choose the best method for a given problem but they will help to inform such a decision. All the computations were carried out using MATHEMATICA version 3.0. In particular this means that all the special functions were available as standard in-built functions.

For the most part the computations focus on one specific value of  $(X/d, Y/d)$ , namely  $(0, 0.01)$ . This point has been chosen for two reasons. First most computations carried out in practice are at  $X = 0$  or for small values of  $X/d$  and these are also the places at which the Green's function is hardest to compute accurately. Secondly, the Green's function can be difficult to compute near to the singularity at  $X = Y = 0$ . The point chosen thus provides a stiff test against which to judge the various methods.

The alternative methods for computing the periodic Green's function described in Section 2 are summarized in Table 1, which also indicates, for each method, the various truncation parameters required in the computation and any restrictions on the permitted values of  $X$  and  $Y$ . Numerical integrations were performed using standard MATHEMATICA packages. Note that the notation  $\sum'_m$  is used to denote the sums in which the  $m = 0$  term is missing.

Computations were carried out for three pairs of values of  $kd$  and  $\beta d$ . First Table 2 displays results for  $kd = 2, \beta d = \sqrt{2}$  which corresponds to an incident wave of wavelength  $\pi d$  at an angle of  $45^\circ$  to the grating, secondly results are given in Table 3 for  $kd = 10, \beta d = 5\sqrt{2}$  which corresponds to an incident wavelength of  $\pi d/5$  at an angle of  $45^\circ$  to the grating and finally Table 4 shows results for  $kd = 2, \beta d = 3$  which corresponds to the problem of determining the frequency of pure Rayleigh–Bloch surface waves along a periodic structure.

For each method an attempt was made to achieve 10 figure accuracy in both the real and imaginary parts and where this was successful the values listed for the truncation parameters are the minimum required (where the numbers are large they represent approximate minimum

values). In any sum of the form  $\sum_{m=-M}^M$  the parameter  $M$  was restricted to be less than or equal to 5000. If 10 figure accuracy was not achieved with a smaller value of  $M$  the value shown is that computed with  $M = 5000$ . In most applications 5 or 6 significant figures will suffice but, as pointed out in [42], the validation of numerical results requires comparisons with benchmarks which should be calculated to a higher degree of accuracy than would normally be needed. The computations were performed on a Power Macintosh 8600/200 and the CPU times shown (which are in units of sixtieths of a second) indicate the relative speed of the various methods.

We will begin by discussing the results shown in Table 2. For the values of  $X/d, Y/d, kd$  and  $\beta d$  used we have  $G_\beta^d = -0.4595298795 - 0.3509130869i$ , to 10 significant figures. The poor convergence of the basic image representation and the basic eigenfunction expansion (methods 1 and 2 respectively) is clear, though it is worth noting that the eigenfunction expansion is superior even though the point at which the Green's function is being evaluated is close to the singularity. The use of Kummer's transformation on the eigenfunction expansion (methods 3 and 4) leads to series which converge significantly faster, though we still need to sum about 1300 terms to achieve 10 figure accuracy. For these methods results are also shown indicating the number of terms required to achieve 6 figure accuracy.

Methods 5 and 6 represent Kummer's transformation applied to the sum of images and the sum in method 6 converges faster than the image sum but still very slowly. As well as the truncation parameters  $M$  and  $N$ , method 5 contains a parameter  $\mu$  which can be varied to alter

Table 1. Alternative forms for the Green's function.

---

$M$	1.	$-\frac{i}{4} \sum_{m=-M}^M H_0(kr_m) e^{im\beta d}$
	2.	$-\frac{1}{2d} \sum_{m=-M}^M \frac{e^{-\gamma_m X } e^{i\beta_m Y}}{\gamma_m}$
$X = 0$ $M, N$	3.	$-\frac{1}{2d} \sum_{m=-M}^M e^{i\beta_m Y} \left( \frac{1}{\gamma_m} - \frac{1}{(\beta_m^2 + k^2)^{\frac{1}{2}}} \right) - \frac{1}{2\pi} \sum_{m=-N}^N K_0(k Y - md) e^{im\beta d}$
$M$	4.	$-\frac{e^{i\beta Y}}{2d} \left( \frac{e^{-\gamma_0 X }}{\gamma_0} + S + \sum_{m=-M}' \left[ \frac{e^{-\gamma_m X }}{\gamma_m} - u_m(X) \right] e^{im\beta Y} \right), \quad S \text{ given by (2.28)}$
$M, N, \mu$	5.	$-\frac{i}{4} \sum_{m=-M}^M [H_0(kr_m) - H_0(k\tilde{r}_m)] e^{im\beta d} - \frac{1}{2d} \sum_{m=-N}^N \frac{e^{-\gamma_m X+\mu d } e^{i\beta_m Y}}{\gamma_m}$
$M$	6.	$-\frac{i}{4} H_0(kr) - \frac{i}{4} \sum_{m=-M}' \left[ H_0(kr_m) - \left( \frac{2}{\pi m kd} \right)^{\frac{1}{2}} e^{i( m kd - \frac{\pi}{4})} \right] e^{im\beta d}$ $-\frac{1+i}{4\pi} \int_0^\infty \left[ \frac{1}{e^{-i(k+\beta)d} - e^{-kdu}} + \frac{1}{e^{-i(k-\beta)d} - e^{-kdu}} \right] \frac{e^{-kdu}}{u^{\frac{1}{2}}} du$

---

Table 1 (continued).

---

$ Y  \leq d$	7.	$-\frac{i}{4}H_0(kr) - \frac{1}{2\pi} \int_0^\infty \left\{ \frac{e^{-ikY} e^{k(Y-d)u}}{e^{-i(\beta+k)d} - e^{-kdu}} + \frac{e^{ikY} e^{-k(Y+d)u}}{e^{i(\beta-k)d} - e^{-kdu}} \right\}$ $\times \frac{\cos[kX(u^2 - 2iu)^{\frac{1}{2}}]}{(u^2 - 2iu)^{\frac{1}{2}}} du$
$ Y  \leq d$	8.	$-\frac{i}{4}H_0(kr) - \frac{1}{2\pi}$ $\times \int_0^\infty \frac{(\cos \beta d - e^{-k\gamma d}) \cosh k\gamma Y + i \sin \beta d \sinh k\gamma Y}{\gamma (\cosh k\gamma d - \cos \beta d)} \cos kXt dt$
$ Y  \leq d$	9.	$-\frac{1}{2\pi} \int_0^\infty \frac{e^{i\beta d \operatorname{sgn}(Y)} \sinh k\gamma  Y  + \sinh k\gamma (d -  Y )}{\gamma (\cosh k\gamma d - \cos \beta d)} \cos kXt dt$
$r < d$ $M, L$	10.	$-\frac{i}{4} \left[ H_0(kr) + \sum_{\ell=0}^L \epsilon_\ell S_\ell J_\ell(kr) \cos \ell \left( \frac{\pi}{2} - \theta \right) \right]$
		$S_0 = -1 - \frac{2i}{\pi} \left[ C + \log \frac{k}{2p} \right] - \frac{2i}{\gamma_0 d} - \frac{2i(k^2 + 2\beta^2)}{p^3 d} \zeta(3)$ $- \frac{2i}{d} \sum_{m=-M}^M \left( \frac{1}{\gamma_m} - \frac{1}{p m } - \frac{k^2 + 2\beta^2}{2p^3  m ^2} \right)$
		$S_{2\ell} = -\frac{2i e^{-2i\ell\theta_0}}{\gamma_0 d} - 2i \sum_{m=1}^M \left\{ \frac{e^{-2i\ell\theta_m}}{\gamma_m d} + \frac{e^{2i\ell\theta_{-m}}}{\gamma_{-m} d} - \frac{(-1)^\ell}{m\pi} \left( \frac{k}{2mp} \right)^{2\ell} \right\}$ $- \frac{2i(-1)^\ell}{\pi} \left( \frac{k}{2p} \right)^{2\ell} \zeta(2\ell + 1) + \frac{i}{\ell\pi}$ $+ \frac{i}{\pi} \sum_{m=1}^{\ell} \frac{(-1)^m 2^{2m} (\ell + m - 1)!}{(2m)! (\ell - m)!} \left( \frac{p}{k} \right)^{2m} B_{2m}(\beta/p)$
		$S_{2\ell-1} = \frac{2i e^{-i(2\ell-1)\theta_0}}{\gamma_0 d}$ $+ 2i \sum_{m=1}^M \left\{ \frac{e^{-i(2\ell-1)\theta_m}}{\gamma_m d} - \frac{e^{i(2\ell-1)\theta_{-m}}}{\gamma_{-m} d} + \frac{i(-1)^\ell \beta d \ell}{m^2 \pi^2} \left( \frac{k}{2mp} \right)^{2\ell-1} \right\}$ $+ \frac{2(-1)^\ell \beta d \ell}{\pi^2} \left( \frac{k}{2p} \right)^{2\ell-1} \zeta(2\ell + 1)$ $- \frac{2}{\pi} \sum_{m=0}^{\ell-1} \frac{(-1)^m 2^{2m} (\ell + m - 1)!}{(2m + 1)! (\ell - m - 1)!} \left( \frac{p}{k} \right)^{2m+1} B_{2m+1}(\beta/p)$
$a, M_1$ $M_2, N$	11.	$-\frac{1}{4} \sum_{m=-M_1}^{M_1} \frac{e^{i\beta_m Y}}{\gamma_m d} \left[ e^{\gamma_m X} \operatorname{erfc} \left( \frac{\gamma_m d}{2a} + \frac{aX}{d} \right) + e^{-\gamma_m X} \operatorname{erfc} \left( \frac{\gamma_m d}{2a} - \frac{aX}{d} \right) \right]$ $- \frac{1}{4\pi} \sum_{m=-M_2}^{M_2} e^{im\beta d} \sum_{n=0}^N \frac{1}{n!} \left( \frac{kd}{2a} \right)^{2n} E_{n+1} \left( \frac{a^2 r_m^2}{d^2} \right)$

---

Table 2. Computed values of  $G_{\beta}^d$  when  $X/d = 0, Y/d = 0.01, kd = 2, \beta d = \sqrt{2}$ . CPU times are in sixtieths of a second.

Method	Parameter values	Computed value	CPU time
1	$M = 5000$	$-0.4634247358 - 0.3530848711i$	1642
2	$M = 5000$	$-0.4595441802 - 0.3509133120i$	1985
3	$M = 650, N = 9$	$-0.4595298795 - 0.3509130869i$	208
4	$M = 60, N = 5$	$-0.4595302867 - 0.3509130662i$	18
	$M = 650$	$-0.4595298795 - 0.3509130869i$	346
	$M = 60$	$-0.4595297998 - 0.3509130799i$	34
5	$M = 5000, N = 300, \mu = 0.01$	$-0.4595298795 - 0.3509130869i$	4517
	$M = 1300, N = 600, \mu = 0.005$	$-0.4595298795 - 0.3509130869i$	1462
	$M = 1000, N = 700, \mu = 0.004$	$-0.4595298795 - 0.3509130869i$	1258
	$M = 5, N = 320, \mu = 0.005$	$-0.4595302671 - 0.3509134879i$	156
6	$M = 5000$	$-0.4595084678 - 0.3509571443i$	1760
7		$-0.4595298800 - 0.3509130868i$	28
8		$-0.4595298795 - 0.3509130869i$	227
9		$-0.4595298794 - 0.3509130869i$	69
10	$M = 80, L = 4$	$-0.4595298795 - 0.3509130869i$	214
	$M = 7, L = 3$	$-0.4595296084 - 0.3509130917i$	55
11	$a = 2, M_1 = 3, M_2 = 2, N = 7$	$-0.4595298795 - 0.3509130869i$	10
	$a = 2, M_1 = 2, M_2 = 1, N = 4$	$-0.4595297462 - 0.3509130866i$	6

the balance between the two sums. Jorgenson and Mitra [17] have carried out computational experiments to determine the optimal value of  $\mu$  in certain situations and they report values of  $\mu$  around 0.02 as being a typically good choice. Results for three values of  $\mu$  are shown here. For  $\mu = 0.01$  we see that the second summation converges much faster than the first and this indicates that  $\mu$  is larger than the optimal value. Decreasing  $\mu$  to 0.005 and then to 0.004 achieves a better balance between the convergence rates of the two summations and the total number of terms required is reduced. The convergence is still poor in comparison to methods based on the eigenfunction expansion. If only 6 figure accuracy is required, then we see that, for small enough  $\mu$ , most of the sum over  $m$  is redundant.

Methods 7, 8 and 9 are integral representations and standard MATHEMATICA packages were used to compute them. The integrand in method 7 has a square root singularity at the origin which presents no difficulties but the integrals in methods 8 and 9 are Cauchy principal-value integrals and have square root singularities at  $t = 1$ . To obtain the desired accuracy it was found necessary to split the range of integration at  $t = 1$  and perform two separate numerical integrations. For these reasons method 7 is the quickest of the three, but the result from this method is slightly inaccurate due to the oscillatory integrand. The loss of accuracy in the 10th figure in method 9 is probably due to the fact that the evaluation point is closed to the singularity at  $X = Y = 0$ , which is not explicit in the formulation.

The convergence of the representation of the Green's function in terms of lattice sums is very rapid indeed, with only 5 terms required, but 80 terms are required to compute the lattice sums themselves to sufficient accuracy. Of course the formulas for the lattice sums could be

Table 3. Computed values of  $G_{\beta}^d$  when  $X/d = 0$ ,  $Y/d = 0.01$ ,  $kd = 10$ ,  $\beta d = 5\sqrt{2}$ . CPU times are in sixtieths of a second.

Method	Parameter values	Computed value	CPU time
1	$M = 5000$	$-0.3547064117 - 0.1764507543i$	2215
2	$M = 5000$	$-0.3538314894 - 0.1769343624i$	1966
3	$M = 1100, N = 7$	$-0.3538172307 - 0.1769332383i$	351
4	$M = 1100$	$-0.3538172307 - 0.1769332383i$	584
5	$M = 600, N = 600, \mu = 0.005$	$-0.3538172307 - 0.1769332384i$	797
6	$M = 5000$	$-0.3538287636 - 0.1769125341i$	2380
7		$-0.3538172309 - 0.1769332385i$	28
8		failed	
9		failed	
10	$M = 300, L = 5$	$-0.3538172307 - 0.1769332383i$	804
11	$a = 1, M_1 = 3, M_2 = 2, N = 78$	$-0.3538185358 - 0.1769332429i$	120
	$a = 2, M_1 = 4, M_2 = 2, N = 28$	$-0.3538172307 - 0.1769332383i$	25
	$a = 3, M_1 = 5, M_2 = 1, N = 18$	$-0.3538172307 - 0.1769332383i$	12
	$a = 4, M_1 = 6, M_2 = 1, N = 13$	$-0.3538172307 - 0.1769332383i$	12
	$a = 5, M_1 = 7, M_2 = 0, N = 11$	$-0.3538172307 - 0.1769332383i$	11
	$a = 6, M_1 = 9, M_2 = 0, N = 9$	$-0.3538172307 - 0.1769332383i$	11
	$a = 7, M_1 = 10, M_2 = 0, N = 8$	$-0.3538172307 - 0.1769332383i$	11
	$a = 8, M_1 = 11, M_2 = 0, N = 8$	$-0.3538172307 - 0.1769332383i$	11
	$a = 9, M_1 = 12, M_2 = 0, N = 7$	$-0.3538172307 - 0.1769332383i$	13
	$a = 10, M_1 = 13, M_2 = 0, N = 7$	$-0.3538172307 - 0.1769332383i$	13

Table 4. Computed values of  $G_{\beta}^d$  when  $X/d = 0$ ,  $Y/d = 0.01$ ,  $kd = 2$ ,  $\beta d = 3$ . CPU times are in sixtieths of a second.

Method	Parameter values	Computed value	CPU time
1	$M = 5000$	$-0.7607250513 - 0.001633152396i$	1658
2	$M = 5000$	$-0.7617606900 - 0.0006391902645i$	1977
3	$M = 1400, N = 12$	$-0.7617463954 - 0.0006387129177i$	429
4	$M = 1500$	$-0.7617463954 - 0.0006387129177i$	811
5	$M = 1200, N = 650, \mu = 0.005$	$-0.7617463956 - 0.0006387129296i$	1419
6	$M = 5000$	$-0.7617785437 - 0.0005770861412i$	1734
7		$-0.7617463953 - 0.0006387134470i$	28
8		$-0.7617463954 - 0.0006387129177i$	219
9		$-0.7617463954 - 0.0006387129177i$	143
10	$M = 200, L = 4$	$-0.7617463954 - 0.0006387129166i$	479
11	$a = 2, M_1 = 3, M_2 = 2, N = 7$	$-0.7617463954 - 0.0006387129177i$	10

accelerated further if required. For a small number of evaluations of the Green's function the lattice sum approach is not as efficient as the integral representations of methods 7 and 9, but since the lattice sums do not depend on the place at which the Green's function is evaluated, and since the vast majority of the time using the method is spent evaluating these sums, the method will become competitive if a sufficient number of evaluations are required for a given  $kd$  and  $\beta d$ . For the values of the parameters considered here, the lattice sum approach becomes competitive with method 7 when the number of evaluations required is greater than about 10. When less accuracy is required we see that the number of terms required to calculate the lattice sums themselves decreases rapidly, but the number of terms in the series for the Green's function does not.

Finally we have Ewald's method which, for the parameter values considered here, is the quickest of all the methods listed in the table. A sensible choice for the parameter  $a$  can be obtained by considering the asymptotics of the two series to be evaluated. It can be shown that, when  $X = 0$ , the terms in the first series behave like  $m^{-2} \exp\{-(m\pi/a)^2\}$ , whereas those in the second series decay like  $m^{-2} \exp\{-(ma)^2\}$ . If we balance the exponentials then  $a \approx \sqrt{\pi}$  is suggested as a reasonable choice. Computations suggest that this approximation underestimates the best value of  $a$  (which of course depends on the values of  $Y/d$ ,  $kd$  and  $\beta d$ ) and  $a = 2$  has been used. A more detailed discussion of the best choice of  $a$  is given below for the higher frequency case, where it matters more. With  $a = 2$  we find that less than 50 terms are required to achieve the desired 10 figure accuracy. For 6 figure accuracy this number is reduced to 20.

Table 3 shows results corresponding to a higher value of  $kd$  (i.e. a higher frequency), but with the same ratio  $k/\beta$ . for this case we have  $G = -0.3538172307 - 0.1769332383i$  to 10 significant figures. Many of the comments made about Table 2 apply here also. As a general rule the Green's function is more difficult to compute in this case, though there are exceptions.

The two methods that rely on computing Cauchy principal-values failed in this case (in which there are now two poles on the real axis), though it may well be possible to use more sophisticated integration techniques to get these methods to work for these parameter values. In view of the results for methods 7 and 11 there seems little point however.

Ewald's method is again the best. The table shows the effect of varying  $a$  in this case and we see that if  $a$  is too small the summation of exponential integrals becomes slowly convergent and accurate results difficult to obtain. The optimum value of  $a$  is somewhere around 6 or 7 though there is little difference in CPU time over the whole range  $3 \leq a \leq 10$ . If more than about 100 evaluations of the Green's function are required, then the lattice sum approach is the most efficient.

An example in which  $\beta > k$  is shown in Table 4. In this case the integrals in methods 8 and 9 are no longer principal-value integrals but they still take considerably longer to evaluate than that in method 7, mainly due to the fact that the integrand still has a square root singularity at  $t = 1$ . Once again Ewald's method is the best of the alternatives unless a large number of evaluations of  $G_\beta^d$  are required.

As  $X/d$  increases from zero methods based on the eigenfunction expansion become progressively better. Table 5 shows how the basic eigenfunction expansion compares with Ewald's method for two values of  $X/d$ , namely 0.1 and 0.5, the value of  $Y/d$  is taken to be 0.5 in both cases and  $kd = 2$ ,  $\beta d = \sqrt{2}$  as in Table 2. It is clear that at  $X/d = 0.1$  the two methods are roughly comparable and that for  $X/d = 0.5$  the eigenfunction expansion is much better. Note that this is the unaccelerated form of the eigenfunction expansion and that we can achieve even faster convergence using method 4, (method 3 is not applicable for  $X/d > 0$ ).

Table 5. Computed values of  $G_{\beta}^d$  when  $Y/d = 0.5$ ,  $kd = 2$ ,  $\beta d = \sqrt{2}$ . CPU times are in sixtieths of a second.

$X/d$	Method	Parameter values	Computed value	CPU time
0.1	2	$M = 32$	$0.3306805081 - 0.1778394385i$	12
	11	$a = 2, M_1 = 2, M_2 = 2, N = 7$	$0.3306805081 - 0.1778394385i$	10
0.5	2	$M = 7$	$0.3596087433 - 0.04626396800i$	3
	11	$a = 2, M_1 = 3, M_2 = 2, N = 7$	$0.3596087433 - 0.04626396800i$	10

## 6. Concluding remarks

In this paper we have summarized the various different analytic techniques that can be used to speed up the numerical evaluation of the two-dimensional Green's function,  $G(X, Y)$ , for the Helmholtz equation in periodic domains. Here  $Y$  is the distance between the source and field points in the direction of periodicity and  $X$  is the separation in the perpendicular direction.

The most obvious way to represent the Green's function is as an image series, but this is hopeless from a numerical point of view. A representation as an eigenfunction expansion was considered next and such an approach is extremely efficient provided  $|X|$  is large, but poor when  $|X|$  is small, which is often the case in applications. When  $|X|$  is small, the convergence of the eigenfunction expansion can be accelerated if Kummer's transformation is applied, and we have shown that significant improvements in performance can be achieved.

A number of different integral representations for  $G$  have also been considered and were found to be very attractive alternatives when  $|X|$  is small. The lattice sum technique, which results from the application of Graf's addition theorem to the image series representation, leads to expressions which take rather long to compute, but which have the distinct advantage that most of the computational effort is expended in computing series coefficients which do not depend on the position at which the Green's function is to be evaluated. Hence, if a large number of evaluations of  $G$  are required, calculations based on lattice sums may be the most appropriate.

Finally, we have considered Ewald summation, a method commonly used in the theory of crystal lattices. It turns out that this technique is particularly well-suited to the problem at hand and provides the most efficient method for the computation of the Green's function, when  $|X|$  is small.

In summary, there are three methods which would seem to be worthy of consideration. If only a small number of evaluations of  $G$  are required, then the eigenfunction expansion (accelerated if necessary) is best for sufficiently large  $|X|$ , whereas in the complementary regime in which  $|X|$  is small, the expression from Ewald's method is the best. If a large number of evaluations are needed, then the lattice sum approach should be considered, though the number of evaluations at which this method becomes quicker than its competitors depends on the parameters  $k$  and  $\beta$ .

Of course, in most applications it is not only the Green's function that is required, but also its first spatial derivative. These can easily be computed from the rapidly convergent expressions for  $G$  given in this paper, simply by differentiating the  $n$  term by term, though



the convergence of the resulting series will not be as good. This is one of the reasons that the Green's function has been computed to such a high accuracy in Section 5, since the same series will be capable of delivering acceptable accuracy for the derivatives of  $G$  in any practical application.

## References

1. R. Petit (ed), *Electromagnetic Theory of Gratings*, volume 22 of *Topics in Current Physics*. Berlin: Springer-Verlag (1980) 284 pp.
2. C. H. Wilcox, *Scattering Theory for Diffraction Gratings*. New York: Springer-Verlag (1984) 163 pp.
3. M. Abramowitz and I. A. Stegun, *Handbook of Mathematical Functions*. New York: Dover (1965) 1046 pp.
4. D. Shanks, Non-linear transformations of divergent and slowly-convergent sequences. *J. Math. Phys.* 34 (1955) 1–42.
5. P. Wynn, On the convergence and stability of the epsilon algorithm. *SIAM J. Num. Anal.* 3 (1966) 91–122.
6. Noyan Kinayman and M. I. Aksun, Comparative study of acceleration techniques for integrals and series in electromagnetic problems. *Radio Science* 30 (1995) 1713–1722.
7. G. Barton, *Elements of Green's Functions and Propagation. Potentials, Diffusion, and Waves*. Oxford: Clarendon Press (1989) 465 pp.
8. D. V. Evans and C. M. Linton, Edge waves along periodic coastlines. *Q. Jl. Mech. Appl. Math.* 46 (1993) 642–656.
9. V. Twersky, On the scattering of waves by an infinite grating. *IRE Trans. on Antennas and Propagation* 4 (1956) 330–345.
10. S. Singh and R. Singh, On the use of  $\rho$ -algorithm in series acceleration. *IEEE Trans. Antennas Propagat.* 39 (1991) 1514–1517.
11. C. M. Linton and D. V. Evans, The radiation and scattering of surface waves by a vertical circular cylinder in a channel. *Phil. Trans. R. Soc. Lond. A* 338 (1992) 325–357.
12. James R. Wait, Reflection from a wire grid parallel to a conducting plane. *Can J. Phys.* 32 (1954) 571–579.
13. R. Lampe, P. Klock and P. Mayes, Integral transforms useful for the accelerated summation of periodic, free-space Green's functions. *IEEE Trans. Microwave Theory Tech.* 33 (1985) 734–736.
14. J. D. Achenbach and Z. L. Li, Reflection and transmission of scalar waves by a periodic array of screens. *Wave Motion* 8 (1986) 225–234.
15. A. E. Heins, The Green's function for periodic structures in diffraction theory with an application to parallel plate media, I. *J. Math. Mech.* 6 (1957) 401–426.
16. P. M. Van den Berg, Diffraction theory of a reflection grating. *Appl. Sci. Res.* 24 (1971) 261–293.
17. Roy E. Jorgenson and Raj Mittra, Efficient calculation of the free-space periodic Green's function. *IEEE Trans. Antennas Propagat.* 38 (1990) 633–642.
18. I. S. Gradshteyn and I. M. Ryzhik, *Tables of Integrals, Series and Products*. New York: Academic Press (1965) 1160pp.
19. N. A. Nicorovici, R. C. McPhedran and R. Petit, Efficient calculation of the Green's function for electromagnetic scattering by gratings. *Phys. Rev. E* 49 (1994) 4563–4577.
20. L. Lewin, *Polylogarithms and Associated Functions*. New York: North Holland (1981) 359 pp.
21. F. Zolla and R. Petit, Sur le calcul de la fonction de Green en théorie des réseaux. In: *OHD'95*. University of Zaragoza (1995).
22. S. Singh, W. F. Richards, J. R. Zinecker, and D. R. Wilton, Accelerating the convergence of series representing the free space periodic Green's function. *IEEE Trans. Antennas Propagat.* 38 (1990) 1958–1962.
23. R. M. Shubair and Y. L. Chow, Efficient computation of the periodic Green's function in layered dielectric media. *IEEE Trans. Microwave Theory Tech.* 41 (1993) 498–502.
24. R. W. Yeung and S. H. Sphaier, Wave-interference effects on a truncated cylinder in a channel. *J. Engng. Math.* 23 (1989) 95–117.
25. A. W. Mathis and A.F. Peterson, A comparison of acceleration procedures for the two-dimensional periodic Green's function. *IEEE Trans. Antennas Propagat.* 44 (1996) 567–571.
26. A. Erdélyi, W. Magnus, F. Oberhettinger, and F. G. Tricomi, *Tables of Integral Transforms*, volume 1. New York: McGraw-Hill (1954) 391 pp.

27. C. M. Linton and D. V. Evans, The interaction of waves with a row of circular cylinders. *J. Fluid Mech.* 251 (1993) 687–708.
28. P. McIver and G. S. Bennett, Scattering of water waves by axisymmetric bodies in a channel. *J. Engng. Math.* 27 (1993) 1–29.
29. R. E. Crandall and J. F. Delford, The potential within a crystal-lattice. *J. Phys. A* 20 (1987) 2279–2292.
30. R. Petit, From functional analysis to the method of fictitious sources in E.M. diffraction. In: *MMET'94*. Kharkov (1994).
31. N. A. Nicorovici and R. C. McPhedran, Lattice sums for off-axis electromagnetic scattering by gratings. *Phys. Rev. E* 50 (1994) 3143–3160.
32. V. Twersky, Elementary function representation of Schlömilch series. *Arch. Rational Mech. Anal.* 8 (1961) 323–332.
33. P. P. Ewald, Die Berechnung optischer und elektrostatischen Gitterpotentiale. *Ann. Phys.* 64 (1921) 253–268.
34. M. Born and Kun Huang, *Dynamical Theory of Crystal Lattices*. The International Series of Monographs on Physics. Oxford: Clarendon Press (1954).
35. K. E. Jordan, G. R. Richter and Ping Sheng, An efficient numerical evaluation of the Green's function for the Helmholtz operator on periodic structures. *J. Comput. Phys.* 63 (1986) 222–235.
36. A. Sugiyama, Method for rapid convergence of lattice sums by the use of Fourier transforms. *J. Phys. Soc. Jpn* 53 (1984) 1624–1633.
37. F. S. Han and B. Segall, Energy bands in periodic lattices—Green's function method. *Phys. Rev.* 124 (1961) 1786–1796.
38. E. T. Whittaker and G. N. Watson, *A Course of Modern Analysis*. Cambridge: Cambridge University Press, 4th edition (1927) 608 pp.
39. W. Gautschi, Efficient computation of the complex error function. *SIAM J. Num. Anal.* 7 (1970) 187–198.
40. D. V. Evans and M. Fernyhough, Edge waves along periodic coastlines. Part 2. *J. Fluid Mech.* 297 (1995) 301–325.
41. C. M. Linton and D. V. Evans, Integral equations for a class of problems concerning obstacles in waveguides. *J. Fluid Mech.* 245 (1992) 349–365.
42. J. N. Newman, Approximation of free-surface Green functions. In: P. A. Martin and G. R. Wickham (eds.), *Wave Asymptotics*. Cambridge University Press (1992) pp. 107–135.